Research Article

Journal of Labelled Compounds and Radiopharmaceuticals

Received 17 September 2007, Revised 1 November 2007, Accepted 30 November 2007 Published online 1 February 2008 in Wiley Interscience

(www.interscience.wiley.com) DOI: 10.1002/jlcr.1494

# Synthesis and biological evaluation of carbon-11-labeled acyclic and furo[2,3-d]pyrimidine derivatives of bicyclic nucleoside analogues (BCNAs) for structure–brain uptake relationship study of BCNA tracers

**Satish K. Chitneni,[a] Jan Balzarini,[b] Sofie Celen,[a] Natalia Dyubankova,[c] Alfons M. Verbruggen,[a] and Guy M. Bormans[a]***

**We reported earlier on radiolabeled alkoxyphenyl bicyclic nucleoside analogues (BCNAs) as potential positron emission tomography (PET) reporter probes for imaging of varicella zoster virus thymidine kinase (VZV-tk) gene *in vivo*. Despite their favorable physicochemical properties, these tracers are not taken up in the brain in mice. In order to probe the role of the deoxyribose sugar moiety in blood-brain barrier (BBB) penetration of these molecules, we have synthesized and evaluated a carbon-11-labeled acyclic bicyclic nucleoside derivative ([$^{11}$C]-10) where the 2′-deoxyribose sugar is replaced with a (2-hydroxyethoxy)methyl group and [$^{11}$C]-12, which has no sugar moiety but a [$^{11}$C]methyl group on the N-3 position of the pyrimidine ring. Methylation was achieved on the phenol ([$^{11}$C]-10) or the N-3 position ([$^{11}$C]-12) using [$^{11}$C]methyl triflate (radiosynthesis). The (non-radioactive) acyclic *O*-methyl derivative 10 has rather poor affinity for the enzyme VZV-TK *in vitro* ($IC_{50}$: 430 μM), compared with the moderate affinity of the BCNA-base *N*-methyl derivative 12 ($IC_{50}$: 79 μM). In normal mice, none of the two tracers ([$^{11}$C]-10 or [$^{11}$C]-12) showed significant uptake in the brain, suggesting that compounds containing a furo[2,3-*d*]pyrimidine system do not cross the BBB.**

**Keywords:** BCNA; VZV-tk; carbon-11; PET; brain uptake

## Introduction

Non-invasive imaging of reporter gene systems using positron emission tomography (PET) or single photon emission tomography (SPECT) offers valuable information about the progress of gene- or cell-based therapy in several diseases including cancer, Parkinson's disease, Alzheimer's disease and stroke.[1–4] Herpes simplex virus type 1 thymidine kinase (HSV1-tk) is the most widely studied reporter gene for which at least 15 different radiolabeled nucleoside analogues have been synthesized and evaluated as substrates.[5–8] These substrates are activated by the protein product of HSV1-tk, which converts them to the mono- and di-phosphate derivatives, and further conversion by cellular kinases results in the formation of tri-phosphate derivatives.[5–10] These phosphorylated metabolites are negatively charged at physiological pH and, hence, can be supposed to remain trapped inside the cells. This entrapment of the radiolabeled substrate in HSV1-tk expressing cells (Note: tk refers to the gene and TK refers to the protein) can be quantitatively detected externally by PET or SPECT imaging, depending on the radioisotope used. However, as none of these tracers for HSV1-tk efficiently crosses the blood-brain barrier (BBB), presumably due to their hydrophilicity, there is a need for lipophilic BBB penetrating tracers, either for the existing reporter genes or as new reporter systems.

Bicyclic nucleoside analogues (BCNAs) are a novel class of antiviral compounds active against varicella zoster virus (VZV). They display a high lipophilicity with calculated log *P* (*C* log *P*) values ranging between 0.4 and 4.6.[11,12] Extensive structure–-activity relationship (SAR) studies have been carried out with respect to their antiviral activity since their discovery by Mc Guigan *et al.*[11] Of all the BCNAs synthesized and evaluated so far, para-alkylphenyl BCNAs represent the most active series, in particular, the *p*-pentyl analogue has a potency of about 10 000 times higher than that of the current anti-VZV drug of choice (acyclovir).[13–15] Because of their lipophilicity, BCNAs were anticipated to efficiently pass through cellular membranes and biological barriers such as the BBB.[14] In addition to their high (anti-VZV) potency, BCNAs also have high specificity for VZV-TK,

[a]*Laboratory for Radiopharmacy, Faculty of Pharmaceutical Sciences, Katholieke Universiteit Leuven, Leuven, Belgium*

[b]*Laboratory for Virology and Chemotherapy, Rega Institute for Medical Research, Katholieke Universiteit Leuven, Leuven, Belgium*

[c]*Laboratory for Medicinal Chemistry, Rega Institute for Medical Research, BioMacs, Katholieke Universiteit Leuven, Leuven, Belgium*

**Correspondence to: Guy M. Bormans, Onderwijs & Navorsing 2, Herestraat 49, bus 821, BE-3000 Leuven, Belgium.*
*E-mail: guy.bormans@pharm.kuleuven.be*

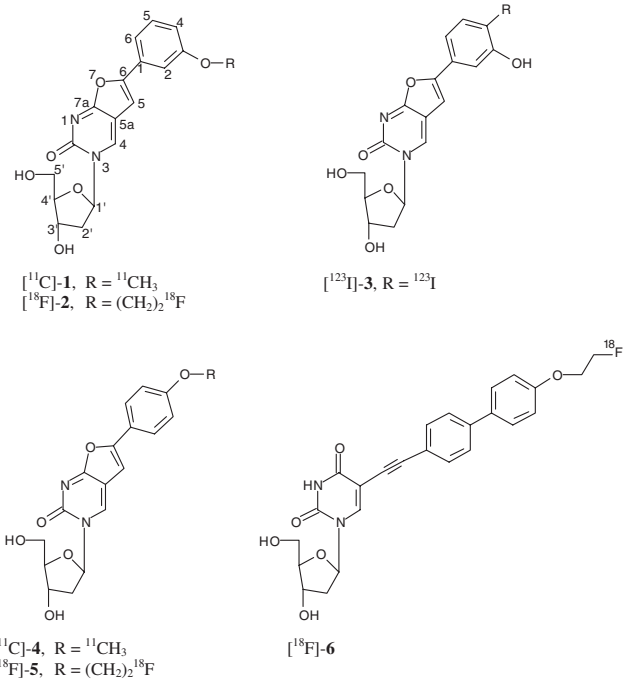


**Figure 1.** Chemical structures of the previously reported radiolabeled BCNAs and a 5-ethynyl-2′-deoxyuridine derivative ([$^{18}$F]-**6**).

**Table 1.** Affinity for VZV-TK and log $P_{7.4}$ values for the previously reported and currently synthesized compounds

| Compound | $IC_{50}$ (μM)[a] | Log $P$[b] | Reference |
|---|---|---|---|
| [$^{11}$C]-**1** | 4.8 ± 1.7 | 1.27 ± 0.04 | 18 |
| [$^{18}$F]-**2** | 53 ± 12 | 1.24 ± 0.03 | 18 |
| [$^{123}$I]-**3** | 4.2 ± 0.6 | 0.83 ± 0.01 | 20 |
| [$^{11}$C]-**4** | 1.5 ± 0.2 | 1.30 ± 0.03 | 19 |
| [$^{18}$F]-**5** | 4.2 ± 0.6 | 1.21 ± 0.02 | 19 |
| [$^{18}$F]-**6** | > 500 | 2.40 ± 0.2 | 21 |
| **9** | 37 ± 8 | — | — |
| [$^{11}$C]-**10** | 430 ± 29 | 1.20 ± 0.01 | — |
| **11** | 64 | — | — |
| [$^{11}$C]-**12** | 79 | 1.18 ± 0.03 | — |

[a]Data are expressed as mean ± SD; $n = 2$; $IC_{50}$ was determined using different concentrations of the non-radioactive BCNA analogue and defined as the 50% inhibitory concentration or compound concentration in μM required to inhibit VZV-TK-catalyzed phosphorylation of 1 μM [$CH_3$-$^3$H]dThd by 50%.
[b]Data are expressed as mean ± SD; $n = 6$.

which converts them to the mono- and di-phosphate derivatives. Interestingly, BCNAs do not have affinity for the closely related HSV1-TK or mammalian cytosolic or mitochondrial TKs.[16,17] The high specificity and the lipophilicity of the BCNAs make them suitable candidates for evaluation as reporter probes, which might cross BBB, for gene expression imaging in the brain.

With this aim, we evaluated the possibility of using radiolabeled BCNAs as PET reporter probes in combination with VZV-tk as reporter gene. We have synthesized fluorine-18- or carbon-11-labeled meta- or para-alkoxyphenyl-BCNA tracers whose chemical structures are presented in Figure 1 and evaluated them in human embryonic kidney cell line HEK-293T cells.[18,19] *In vitro* enzymatic assays using non-radioactive compounds and purified VZV-TK have revealed that the affinity of meta-alkoxyphenyl BCNAs for VZV-TK decreases as the alkyl chain length increases (see Table 1), which was further evident in cell uptake experiments using [$^{11}$C]-**1** and [$^{18}$F]-**2**.

In contrast to the meta-fluoroethoxyphenyl-BCNA ([$^{18}$F]-**2**), the para-compound ([$^{18}$F]-**5**) has good affinity for the enzyme ($IC_{50}$ of 4.2 μM vs 53 μM for the meta-compound; Table 1). Indeed, [$^{18}$F]-**5** showed good uptake in cell studies with uptake ratios similar as those of [$^{11}$C]-**1**, with about 54-fold higher accumulation in VZV-tk expressing cells than in control cells.[19]

We also synthesized an iodine-123-labeled BCNA ([$^{123}$I]-**3**) for SPECT and evaluated its accumulation in VZV-tk expressing 293T cells.[20] In spite of its comparable affinity for VZV-TK ($IC_{50}$: 4.2 μM; Table 1) its uptake ratio (VZV-TK cells/control cells) was not more than 1.74, which is about 30 times less than that of [$^{11}$C]-**1** and [$^{18}$F]-**5**. This low accumulation is probably due to the higher hydrophilicity of [$^{123}$I]-**3**, which is evident from its lower log $P$ value (see Table 1). Similarly, none of the BCNA tracers synthesized so far had significant brain uptake in biodistribution studies in normal mice, although they fulfill the theoretical requirements for passive diffusion of such molecules through the BBB. Further, we synthesized the fluorine-18-labeled 5-ethynyl-2′-deoxyuridine derivative [$^{18}$F]-**6**, which is a BCNA precursor (non-cyclized BCNA) and is very lipophilic (log $P$: 2.4; Table 1) compared with the intact BCNA tracers.[21] However, brain uptake was minimal for this tracer too. On the basis of the results of these biodistribution studies of BCNA tracers, we hypothesized that the presence of the polar sugar moiety in the chemical structure might be detrimental for the BBB passage of this class of molecules, irrespective of the overall lipophilicity. In order to examine this hypothesis, we now synthesized a carbon-11-labeled acyclic-BCNA tracer [$^{11}$C]-**10**, which has a hydroxyethoxymethyl side chain instead of a 2′-deoxy ribose sugar for BCNAs, and also a carbon-11-labeled BCNA without a sugar moiety ([$^{11}$C]-**12**). We chose to synthesize acyclic BCNAs bearing at the C-6 position of the furopyrimidine system a phenyl ring instead of alkyl or alkyn-1-yl as a substituent[22] as they can be easily compared with the previously reported BCNA tracers[18–20] and to use a phenol as a precursor for radiolabeling. This paper reports the chemical and radiochemical synthesis of [$^{11}$C]-**10** and [$^{11}$C]-**12**, their *in vitro* affinity data, and biodistribution studies in normal mice.

## Results and discussion

### Chemistry

Precursors **9** and **11** for radiolabeling were synthesized by a Sonogashira coupling of 1-[(2-hydroxyethoxy)methyl]-5-iodouracil (**8**) and 5-iodouracil (**7**), respectively, with 3-hydroxyphenyl acetylene, followed by *in situ* cyclization of the reaction products. First, compound **8** was synthesized by linking a 2-hydroxyethoxymethyl chain to the N-1 of 5-iodouracil (**7**).[23] For this purpose, **7** was first protected by treatment with bis(trimethylsilyl)acetamide (BSA) to give 2,4-bis(trimethylsilyl)-5-iodouracil followed by the addition of 1,3-dioxolane, chlorotrimethylsilane, and potassium iodide for the generation of the iodomethyl[(trimethylsilyl)oxy]ethyl ether *in situ*. Subsequent



  

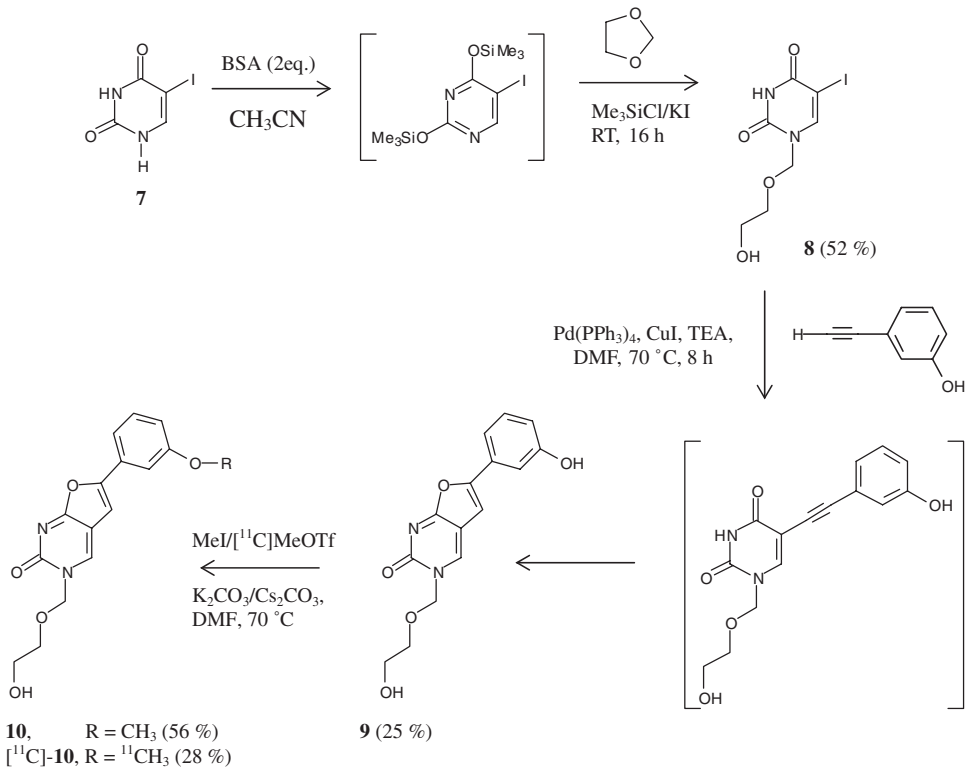


**Figure 2.** Synthesis of radiolabeling precursor **9** and its non-radioactive or radioactive *O*-methyl derivative **10** (BSA = *N*,*O*-bis(trimethylsilyl)acetamide).

reaction with 2,4-bis(trimethylsilyl)-5-iodouracil yielded compound **8** (Figure 2). Compound **8** was then coupled to 3-hydroxyphenyl acetylene under co-catalysis of Pd and cuprous ions followed by cyclization of the intermediate in a one-pot synthesis *via* the procedure reported by Janeba *et al.*[22] to obtain the fluorescent compound **9** in moderate yield (25%). Compound **11** was also synthesized following the coupling reaction analogous to the synthesis of **9** but starting from 5-iodouracil (**7**) instead of compound **8**, in 44% yield (Figure 3). The relatively lower yield of compound **9** was mainly due to the cleavage of the *N*-3-hydroxyethoxymethyl chain during the reaction, resulting in the eventual formation of compound **11** as a side product.

Compounds **9** and **11** were used as precursors for stable non-radioactive methoxy compounds **10** and **12**, respectively. Methylation of **9** and **11** was achieved by heating the respective precursors with methyl iodide (MeI) in the presence of $K_2CO_3$ in DMF at 70°C for 1 h,[18] in 56 and 32% yield, respectively. In the $^1$H NMR spectrum of the reaction product of the methylation of **9**, the absence of a signal (δ 9.75) corresponding to the phenol group and the presence of a sharp singlet (δ 3.83) from the methyl ether support a successful *O*-methylation, yielding compound **10**. We anticipated that the methylation of **11** would also occur preferentially at the phenol group, due to the higher reactivity of a phenol in its deprotonated form in the presence of the base ($K_2CO_3$), than at the N-3 of the furopyrimidine system. However, the $^1$H NMR spectrum of the reaction product after methylation of **11** revealed the absence of the NH proton at 12.11 ppm and the presence of a signal corresponding to the phenol (δ 9.73), suggesting that *N*-methylation rather than the *O*-methylation occurred in these reaction conditions. Further, 2D NMR ($^1$H-$^{13}$C) analysis was performed on the phenol precursor **11** and its methylated product **12** in heteronuclear single quantum correlation (HSQC) experiments and heteronuclear multiple bond correlation (HMBC) experiments. Based on HSQC analysis, C-4 (furopyrimidine) and phenol carbons were undoubtedly assigned. According to the HMBC spectrum of **11**, the hydroxyl group of the phenyl moiety at 9.73 has long range couplings with C-2, C-3 and C-4 carbons (phenyl moiety). A similar interaction has been observed for the proton at 9.73 ppm for compound **12** also, indicating the presence of a free hydroxyl group on C-3 position of the phenyl ring. These data strongly suggest that the methylation indeed occurred at the N-3 position of the pyrimidine ring, resulting in compound **12** as shown in Figure 4. Reversed phase-high-performance liquid chromatography (RP-HPLC) analysis of methylation reaction mixture of **11** has shown the presence of another mono-methyl isomer (as determined using mass spectrometry), presumably the *O*-methyl derivative, which was not isolated and characterized due to its relatively low amount (about 4%).

## Radiochemistry

Radiolabeling of **9** was initially performed by heating 0.2 mg of the precursor with [$^{11}$C]MeI in the presence of $Cs_2CO_3$ (about 1 mg) in DMF at 70°C for 8 min.[18] However, this reaction resulted in a low radiochemical yield (about 5%). Further optimization of reaction conditions was not tried as increase in reaction time and/or temperature may result in the cleavage of the (2-hydroxyethoxy)methyl chain. Instead, [$^{11}$C]methyl triflate ([$^{11}$C]MeOTf), which is a more powerful methylation reagent

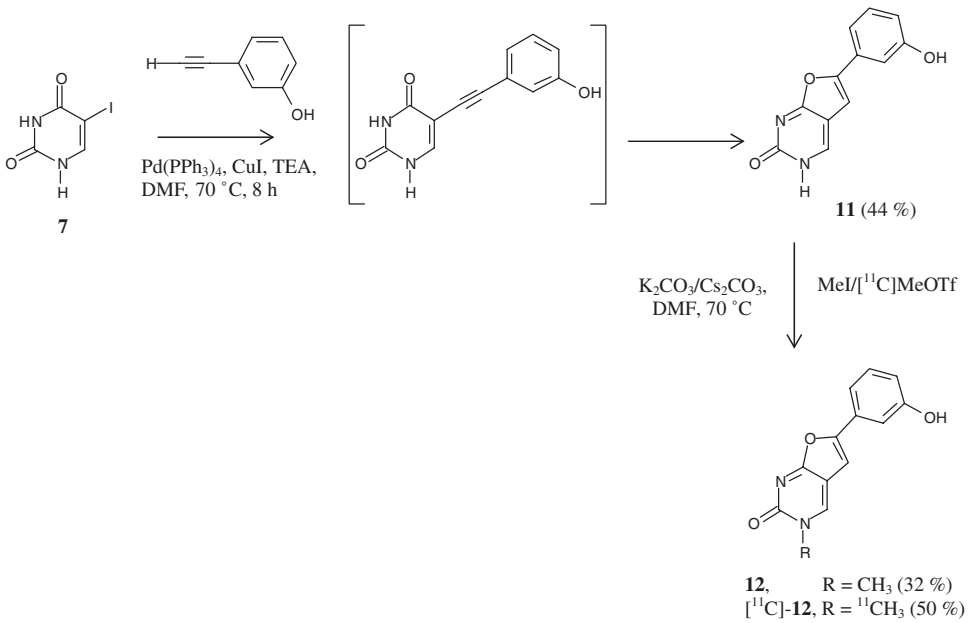


**Figure 3.** Synthesis of radiolabeling precursor **11** and its non-radioactive or radioactive *N*-methyl derivative **12**.

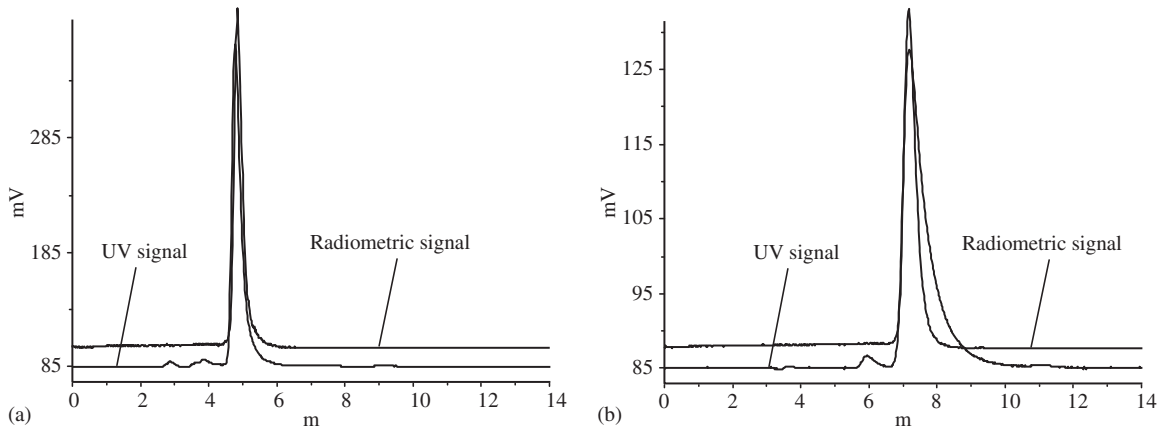


**Figure 4.** RP-HPLC chromatograms of [$^{11}$C]-**10** (A; Rt = 4.5 min) and [$^{11}$C]-**12** (B; Rt = 7.1 min) co-injected with their authentic non-radioactive analogues.

than the [$^{11}$C]MeI, was used for radiolabeling and a methylation yield of 28% was obtained. Radiolabeling of **11** was also performed starting from [$^{11}$C]MeOTf to provide [$^{11}$C]-**12** with a yield of 50%. Both tracers were purified by semi-preparative RP-HPLC. The identity of the tracers was confirmed by co-injection with their authentic non-radioactive analogues on an analytical RP-HPLC system (Figure 4). The radiochemical purity (RCP) after isolation by HPLC was found to be >99% for both the tracers.

## Lipophilicity of the tracers

The lipophilicity of the RP-HPLC purified radiolabeled products [$^{11}$C]-**10** and [$^{11}$C]-**12** was determined by partitioning between 1-octanol and 0.025 M phosphate buffer pH 7.4 ($n = 6$; Table 1). For comparison, the log *P* values of previously synthesized BCNAs tracers are also presented in the same table. We anticipated [$^{11}$C]-**10** and [$^{11}$C]-**12** to be more lipophilic than the previously reported intact BCNA tracers (Figure 1), but the log *P* value of 1.2 for both tracers indicates that the modifications of the 2′-deoxyribose sugar moiety do not significantly alter the lipophilicity of the BCNAs. Compound [$^{11}$C]-**12** appeared to be even less lipophilic than the acyclic-BCNA tracer [$^{11}$C]-**10** as its elution from an RP-C18 HPLC column required an about 10% lower concentration of EtOH in the mobile phase for a similar retention time (Rt). However, this was not reflected in its partition coefficient as there was no significant difference between the log *P* values of [$^{11}$C]-**10** and [$^{11}$C]-**12**. In general, these log *P* values are similar or comparable to those of the previously synthesized intact BCNA tracers and are within the optimal range (0.9–2.5) for passive diffusion of a neutral compound over the BBB.[24]

## Biodistribution and brain uptake of the tracers

The biodistribution of [$^{11}$C]-**10** and [$^{11}$C]-**12** at 2 and 60 min post injection (p.i.) was evaluated in normal male NMRI mice and the results are presented in Tables 2 and 3 as percentage of injected dose (% ID) and as standard uptake values (SUVs) for selected organs. SUVs were calculated as (radioactivity in cpm in organ/weight of the organ)/(total counts recovered/body weight). The *in vivo* distribution and excretion of [$^{11}$C]-**10** are similar to that of

**Table 2.** Biodistribution of [$^{11}$C]-**10** in normal mice at 2 and 60 min p.i.

| Organ | %ID[a] | | SUV[b] | |
|---|---|---|---|---|
| | 2 min | 60 min | 2 min | 60 min |
| Urine | 1.7 ± 1.0 | 30.6 ± 2.3 | — | — |
| Kidneys | 11.6 ± 1.2 | 0.7 ± 0.1 | 6.2 ± 0.6 | 0.4 ± 0.1 |
| Liver | 29.3 ± 1.7 | 6.2 ± 1.4 | 5.1 ± 0.4 | 1.4 ± 0.2 |
| Spleen + pancreas | 1.6 ± 0.5 | 0.3 ± 0.1 | 1.8 ± 0.3 | 0.3 ± 0.1 |
| Lungs | 1.2 ± 0.0 | 0.1 ± 0.0 | 1.6 ± 0.2 | 0.2 ± 0.0 |
| Heart | 0.9 ± 0.1 | 0.0 ± 0.0 | 1.9 ± 0.2 | 0.1 ± 0.0 |
| Stomach | 1.2 ± 0.1 | 0.6 ± 0.1 | — | — |
| Intestines | 15.2 ± 2.3 | 55.4 ± 1.4 | — | — |
| Brain | 0.1 ± 0.0 | 0.1 ± 0.0 | 0.2 ± 0.0 | 0.1 ± 0.0 |
| Blood | 7.9 ± 0.4 | 1.0 ± 0.1 | 1.1 ± 0.1 | 0.1 ± 0.0 |
| Carcass | 27.0 ± 2.1 | 5.3 ± 0.4 | — | — |

*Note*: Data are expressed as mean ± SD; $n = 3$ per time point.
[a]Percentage of injected dose calculated as cpm in organ/total cpm recovered.
[b]Standard uptake values calculated as (radioactivity in cpm in organ/weight of the organ in g)/(total counts recovered/body weight in g).

**Table 3.** Biodistribution of [$^{11}$C]-**12** in normal mice at 2 and 60 min p.i.

| Organ | %ID[a] | | SUV[b] | |
|---|---|---|---|---|
| | 2 min | 60 min | 2 min | 60 min |
| Urine | 20.5 ± 1.5 | 45.2 ± 0.8 | — | — |
| Kidneys | 7.3 ± 0.5 | 0.1 ± 0.0 | 4.5 ± 0.2 | 0.1 ± 0.0 |
| Liver | 21.1 ± 0.7 | 3.0 ± 3.4 | 3.6 ± 0.2 | 0.5 ± 0.5 |
| Spleen + pancreas | 1.1 ± 0.3 | 0.0 ± 0.0 | 1.5 ± 0.3 | 0.0 ± 0.0 |
| Lungs | 0.5 ± 0.1 | 0.0 ± 0.0 | 0.7 ± 0.1 | 0.0 ± 0.0 |
| Heart | 0.3 ± 0.0 | 0.0 ± 0.0 | 0.7 ± 0.0 | 0.0 ± 0.0 |
| Stomach | 0.5 ± 0.2 | 0.2 ± 0.1 | — | — |
| Intestines | 24.5 ± 2.7 | 47.9 ± 3.1 | — | — |
| Brain | 0.0 ± 0.0 | 0.0 ± 0.0 | 0.1 ± 0.0 | 0.0 ± 0.0 |
| Blood | 3.7 ± 1.0 | 0.1 ± 0.0 | 0.5 ± 0.1 | 0.0 ± 0.0 |
| Carcass | 19.9 ± 3.7 | 3.0 ± 1.1 | — | — |

*Note*: Data are expressed as mean ± SD; $n = 3$ per time point.
[a]Percentage of injected dose calculated as cpm in organ/total cpm recovered.
[b]Standard uptake values calculated as (radioactivity in cpm in organ/weight of the organ in g)/(total counts recovered/body weight in g).

the previously reported BCNA tracers[18–20] with about 55% ID excreted into the intestines and 31% ID into the urine at 60 min p.i. On the other hand, [$^{11}$C]-**12** was cleared almost equally via the intestines (48% ID at 60 min p.i.) and kidneys (45% ID). The clearance of both tracers from blood was rapid with ⩽1.0% ID remaining in blood at 60 min p.i. Except for liver (3–6% ID) and intestines (48–55% ID), the radioactivity in other major organs was negligible 60 min after injection of the tracers. At 2 min p.i., the highest concentration of radioactivity was found in the kidneys with a SUV of 6.2 for [$^{11}$C]-**10** and 4.5 for [$^{11}$C]-**12**. This was succeeded by the liver with SUVs of 5.1 for [$^{11}$C]-**10** and 3.6 for [$^{11}$C]-**12**. At 60 min p.i., these values were 1.4 or less for [$^{11}$C]-**10**, and 0.5 or less for [$^{11}$C]-**12**. This indicates a good clearance of the tracers from blood and major organs.

[$^{11}$C]-**10** and [$^{11}$C]-**12** were synthesized with the aim to evaluate their brain uptake for a better understanding whether the presence of a ribose/deoxyribose sugar is required for affinity for the VZV-TK and how its absence influences BBB penetration of such nucleoside analogues. It is generally accepted that for a passive diffusion of a compound over the BBB, its log *P* value should be between 0.9 and 2.5, its molecular mass less than 650 Da, and the compound should be uncharged at physiological pH.[24–26] The log *P* of [$^{11}$C]-**10** and [$^{11}$C]-**12** is about 1.2, both compounds are uncharged at physiological pH, and their molecular mass is 316 and 242 Da, respectively. Despite these favorable characteristics, none of these two tracers showed significant brain uptake (0.04–0.1% ID at 2 min p.i.), similar to the previously synthesized BCNA tracers.[18–20] This seems to indicate that a furopyrimidine base system is unable to diffuse over the BBB, irrespective of the presence or the absence of a sugar moiety. Lack of brain uptake for the radiolabeled BCNA precursor [$^{18}$F]-**6** (log *P*: 2.4)[21] further suggests the uracil base as the entity responsible for the failure of such molecules to cross the BBB. However, this does not exclude an active efflux (from the endothelium of the BBB back to blood) as potential underlying mechanism for the failed efficient transport of these tracers across the BBB.[27] Several multispecific transport proteins have been identified as mediators of efflux in the BBB, including P-glycoprotein (P-gp) and the multi-drug-resistance associated protein (MRP) whose function determines cerebral uptake of many drugs. Biodistribution of the tracers after pretreatment of the animals with a specific substrate of the efflux protein can confirm whether or not the test drug is a substrate for that efflux protein.[27] However, the negligible initial uptake (0.04–0.1% ID in brain at 2 min p.i.)[18–20] suggests that the active efflux mechanism might not be the predominant mechanism involved in the poor penetration of the BCNA tracers over the BBB.

### Affinity for the VZV-TK enzyme *in vitro*

The affinity of the synthesized compounds (non-radioactive) for the nucleoside kinase enzyme was examined using purified recombinant VZV-TK in the presence of tritiated dThd (1 μM) as the natural substrate, and the results are expressed as 50% inhibitory concentration ($IC_{50}$) values in Table 1. For comparison, the $IC_{50}$ values of the previously reported BCNA tracers are also given in Table 1. The acyclic BCNA phenol precursor **9** showed moderate affinity ($IC_{50}$: 37 μM) for the enzyme, whereas its *O*-methyl derivative **10** has rather poor affinity with an $IC_{50}$ value of 430 μM. The moderate affinity of compound **9** suggests the potential usefulness of acyclic BCNAs as inhibitors of VZV-TK as structural modification may further enhance the observed affinity for VZV-TK. To be a useful tracer for gene expression imaging in the brain, the BCNA tracer agent should have a reasonable initial uptake in the brain and have a good affinity and be a substrate for phosphorylation by the VZV-TK enzyme. Therefore, radiolabeled acyclic BCNAs may not offer additional advantages over the previously reported intact BCNA tracers as they too do not show passage over the BBB. Compounds **11** and **12**, i.e. the 6-(3-hydroxy)phenyl-furo[2,3-*d*]pyrimidin-2(3*H*)-one precursor and its *N*-methyl derivative, respectively, were anticipated not to have any affinity for the enzyme VZV-TK

due to the absence of a 5′-hydroxyl group or deoxyribose sugar that is required for the phosphorylation of these molecules. Hence, the moderate affinity values ($IC_{50}$ **11**: 64 μM; $IC_{50}$ **12**: 79 μM) observed for these two compounds suggest that they bind to the enzyme without being a substrate, thereby inhibiting the phosphorylation of [$CH_3$-$^3$H]deoxythymidine, which was used as a natural substrate for the VZV-TK in the competition experiments. Radiolabeled **12** is probably not a useful tracer for VZV-tk detection *in vivo* because it cannot be phosphorylated and hence will not accumulate inside the VZV-tk expressing cells because of the presence of an ionized phosphate group.

## Experimental

### Instruments, chemicals and general conditions

A Cyclone 18/9 cyclotron (Ion Beam Applications, Louvain-la-Neuve, Belgium) was used for the production of carbon-11. $^1$H NMR spectra were recorded on a Gemini 300 MHz spectrometer (Varian, Palo Alto, USA) using DMSO-$d_6$ as a solvent. HSQC and HMBC spectra for compounds **11** and **12** were recorded on a Bruker Avance 600 MHz NMR spectrometer (Bruker BioSpin, Rheinstetten, Germany). The 2D $^1$H/$^{13}$C correlation via double inept transfer (HSQC) was acquired in a phase-sensitive mode with Echo-Antiecho gradient selection. The 2D $^1$H/$^{13}$C correlation via heteronuclear zero and double quantum coherence (HMBC) was acquired using gradient pulses for selection. The 2D NMR data were processed with Bruker-TopSpin software (Bruker BioSpin). Accurate mass determination was performed on a time-of-flight mass spectrometer (LCT, Micromass, Manchester, UK) equipped with an orthogonal electrospray ionization (ESI) interface, operated in positive mode (ES+) or negative mode (ES−). Samples were infused in acetonitrile/water using a Harvard 22 syringe pump (Harvard instruments, MA, USA). Acquisition and processing of data was done using Masslynx™ software (version 3.5, Waters). HPLC purification was performed using a Merck Hitachi L6200 intelligent pump (Hitachi, Tokyo, Japan) or a Waters 600 pump (Waters, Milford, USA) connected to a UV spectrometer (Waters 2487 Dual λ absorbance detector) set at 254 nm. For the purification and analysis of radiolabeled compounds, the HPLC eluate was passed through a UV detector followed by a radiometric detector connected to a single channel analyzer (Medi-Lab Select, Mechelen, Belgium). Radioactivity measurements during log *P* determination and biodistribution studies were done using an automated gamma counter (3-in NaI(Tl) well crystal) coupled to a multi-channel analyzer (Wallac 1480 Wizard™ 3″, Wallac, Turku, Finland). The results were corrected for background radiation and physical decay during counting. All reagents and solvents were obtained commercially from Acros Organics (Geel, Belgium) or Aldrich, Fluka, Sigma (Sigma-Aldrich, Bornem, Belgium) or Fischer Bioblock Scientific (Tournai, Belgium).

### Chemistry

*1-[(2-Hydroxyethoxy)methyl]-5-iodouracil* ***8***

To a suspension of 5-iodouracil (**7**, 2.38 g, 10 mmol) in acetonitrile (15 mL) was added *N,O*-BSA (5.4 mL, 22 mmol) and the mixture was stirred to obtain a clear solution. To this solution, 1,3-dioxolane (0.7 mL, 10 mmol), potassium iodide (1.7 g, 10 mmol) and chlorotrimethylsilane (1.38 mL, 10 mmol) were sequentially added, and the mixture was stirred at room temperature (RT) for 16 h. The reaction was quenched by the addition of methanol (20 mL) followed by neutralization with sodium bicarbonate (4 g). Solids were removed by filtration and the filtrate was concentrated under reduced pressure. The crude product was purified using column chromatography on silica gel eluted with gradient mixtures of $CH_3OH$ in $CH_2Cl_2$ (up to 8%) to give 1.63 g of compound **8** as a white solid (52% yield). $^1$H NMR (300 MHz, DMSO-$d_6$) δ: 11.70 (brs, 1H), 8.24 (s, 1H), 5.08 (s, 2H), 4.68 (t, $^3J$ = 5.1 Hz, 1H), 3.50–3.46 (m, 4H).

*6-(3-Hydroxy)phenyl-3-[(2-hydroxyethoxy)methyl]furo[2,3-*d*]pyrimidin-2(3*H*)-one* ***9***

To a stirred suspension of compound **8** (1.24 g, 3.99 mmol), tetrakis(triphenylphosphine)palladium(0) (0.23 g, 0.2 mmol) and copper(I) iodide (0.76 g, 3.98 mmol) in DMF (80 mL) under $N_2$ at RT was added 3-hydroxyphenylacetylene (0.57 g, 4.78 mmol) and dry triethylamine (4 mL). The reaction mixture was stirred at 70°C for 8 h followed by the evaporation of solvents under reduced pressure. The crude product was treated with toluene (2 × 20 mL) and the volatiles were evaporated under reduced pressure. The resulting residue was then extracted with hot methanol, and the suspension was filtered and washed with methanol. After concentration of the combined filtrate under reduced pressure, the residue was adsorbed on silica gel and purified using a silica gel column chromatography eluted with gradient mixtures of $CH_3OH$ (up to 10%) in $CH_2Cl_2$. Appropriate fractions were combined and evaporated to yield 0.3 g of a light-yellow solid (25% yield). $^1$H NMR (300 MHz, DMSO-$d_6$) δ: 9.75 (s, 1H), 8.64 (s, 1H), 7.27 (m, 2H), 7.20 (s, 1H), 7.19 (m, 1H), 6.82 (m, 1H), 5.39 (s, 2H), 4.71 (s, 1H), 3.60 (m, 2H), 3.51 (m, 2H). HRMS ESI+: Theor. mass $[C_{15}H_{14}N_2O_5+Na]^+$: 325.0800; found 325.0801.

*6-(3-Methoxy)phenyl-3-[(2-hydroxyethoxy)methyl]furo[2,3-*d*]pyrimidin-2(3*H*)-one* ***10***

To a stirred solution of **9** (50 mg, 0.165 mmol) in DMF (8 mL) was added $K_2CO_3$ (23 mg, 0.165 mmol) and methyl iodide (10 μL, 0.165 mmol). The reaction mixture was stirred at 70°C for 1 h and purified by HPLC using a C-18 semi-preparative column (Econosphere, 10 mm × 250 mm; Alltech, Deerfield, USA) eluted with water–acetonitrile (75:25, V/V) at a flow rate of 3 mL/min (Rt = 15.2 min). After evaporation of the solvent, the methylated product was obtained as a white solid (29 mg, 56%). $^1$H NMR (300 MHz, DMSO-$d_6$) δ: 8.69 (s, 1H), 7.41 (m, 2H), 7.36 (m, 2H), 7.01 (m, 1H), 5.39 (s, 2H), 4.73 (s, 1H), 3.83 (s, 3H), 3.60 (m, 2H), 3.51 (m, 2H). HRMS ESI+: Theor. mass $[C_{16}H_{16}N_2O_5+Na]^+$: 339.0957; found 339.0950.

*6-(3-Hydroxy)phenyl-furo[2,3-*d*]pyrimidin-2(3*H*)-one* ***11***

Compound **11** was synthesized in the same manner as compound **9** but starting from 5-iodouracil **7** (1.19 g; 5 mmol) instead of compound **8**. The crude product was purified using a silica gel column eluted with gradient mixtures of $CH_3OH$ in $CH_2Cl_2$ (up to 10%). The resulting residue was treated with hot acetonitrile followed by filtration to yield the product as yellow solid (0.5 g, 44%). NMR: $\delta_H$ (300 MHz, DMSO-$d_6$) 12.11 (brs, 1H), 9.73 (s, 1H), 8.32 (s, 1H), 7.27 (m, 2H), 7.17 (s, 1H), 7.12 (s, 1H), 6.81 (m, 1H); $\delta_C$ (600 MHz, DMSO-$d_6$) 172.30, 158.27, 156.34,

153.72, 140.91, 130.71, 130.06, 116.94, 115.89, 111.39, 106.94, 99.82. HRMS ESI-: Theor. mass $[C_{12}H_8N_2O_3 - H]^-$: 227.0457; found 227.0464.

*6-(3-Methoxy)phenyl-furo[2,3-*d*]pyrimidin-2(3*H*)-one* ***12***

Compound **12** was synthesized in the same manner as that of **10** but using compound **11** (50 mg, 0.22 mmol) as a starting material. The reaction mixture was purified in a similar manner using water–acetonitrile (85:15, V/V) at a flow rate of 2.5 mL/min (Rt = 19.6 min). After evaporation of the solvent, the methylated product was obtained as a white solid (17 mg, 32%). NMR: $\delta_H$ (300 MHz, DMSO-$d_6$) 9.73 (s, 1H), 8.64 (s, 1H), 7.30 (m, 2H), 7.20 (s, 1H), 7.18 (s, 1H), 6.82 (m, 1H), 3.53 (s, 3H); $\delta_C$ (600 MHz, DMSO-$d_6$) 171.57, 158.27, 155.47, 153.72, 144.39, 130.71, 130.06, 116.93, 115.88, 111.38, 106.84, 99.68, 55.79. HRMS ESI-: Theor. mass $[C_{13}H_{10}N_2O_3 - H]^-$: 241.0613; found 241.0634.

## Radochemistry

*Production of [$^{11}$C]methyl triflate ([$^{11}$C]MeOTf)*

Carbon-11 was produced by a $^{14}N(p,\alpha)^{11}C$ nuclear reaction. The target gas (a mixture of 95% $N_2$ and 5% $H_2$) was irradiated using 18-MeV protons from a Cyclone 18/9 cyclotron (Ion Beam Applications, Louvain-la-Neuve, Belgium) at a beam current of 25 μA for about 30 min to yield [$^{11}$C]$CH_4$. This was then reacted with vaporous $I_2$ at 650°C to convert it to [$^{11}$C]methyl iodide ([$^{11}$C]MeI). The resulting volatile [$^{11}$C]MeI was passed through a glass column (3 mm × 150 mm) containing silvertriflate (AgOTf), which was heated at 275–290°C to yield [$^{11}$C]MeOTf.

*Synthesis of [$^{11}$C]-**10***

The [$^{11}$C]MeOTf resulting from the above reaction was trapped in a reaction vial containing a mixture of **9** (0.2 mg) and $Cs_2CO_3$ (about 1 mg) in anhydrous DMF (0.2 mL). When maximum radioactivity was trapped, the reaction mixture was heated at 70°C for 8 min. The crude reaction mixture was diluted with water (1.6 mL) and applied onto a semi-preparative HPLC column (HS HyperPrep RP $C_{18}$, 100 Å, 8 μm; 10 mm × 250 mm; Alltech), which was eluted with 0.05 M sodium acetate buffer (pH = 5.5)/EtOH (65:35, V/V) at a flow rate of 3 mL/min (Rt = 11.5 min). The identity and purity of the labeled product was analyzed using RP-HPLC on an XTerra™ RP $C_{18}$ column (5 μm, 4.6 mm × 250 mm; Waters), eluted with 0.05 M sodium acetate buffer (pH = 5.5)/acetonitrile (65:35, V/V) at a flow rate of 1 mL/min (Rt = 4.5 min). [$^{11}$C]-**10** was synthesized in 28% radiochemical yield (RCY; relative to [$^{11}$C]MeOTf radioactivity, non-decay corrected (NDC)) and the specific radioactivity was 175.6 GBq/μmol (4.74 Ci/μmol) at the end of synthesis (EOS) (Figure 2).

*Synthesis of [$^{11}$C]-**12***

[$^{11}$C]-**12** was also synthesized in the same manner as that of [$^{11}$C]-**10** but using compound **11** as a precursor, and purification of the product was done using 0.05 M sodium acetate buffer (pH = 5.5)/EtOH (75:25, V/V) as a mobile phase at a flow rate of 3 mL/min (Rt = 13.3 min). The identity and purity analysis of the tracer was performed on analytical XTerra™ RP $C_{18}$ column (Waters) eluted with 0.05 M sodium acetate buffer (pH = 5.5)/acetonitrile (75:25, V/V) at a flow rate of 1 mL/min (Rt = 7.1 min). The RCY of the tracer was 50% (relative to [$^{11}$C]MeOTf radioactivity, NDC) and the specific radioactivity was 68.9 GBq/μmol (1.86 Ci/μmol) at EOS (Figure 3).

## Partition coefficient determination

An aliquot of 25 μL of RP-HPLC purified radiolabeled product containing approximately 550 kBq of [$^{11}$C]-**10** or [$^{11}$C]-**12** was added to a tube containing a mixture of 1-octanol and 0.025 M phosphate buffer pH 7.4 (2 mL each). The tube was vortexed at RT for 2 min followed by centrifugation at 3000 rpm (1837*g*) for 5 min (Eppendorf centrifuge 5810, Eppendorf, Westbury, NY). Aliquots of about 60 and 500 μL were drawn from the 1-octanol and aqueous phases, respectively, taking care to avoid cross-contamination between the two phases, and weighed. The radioactivity in the aliquots was counted using a automated gamma counter. After correcting for density and the mass difference between the two phases, the partition coefficient (*P*) was calculated as (radioactivity (cpm/mL) in 1-octanol)/(radioactivity (cpm/mL) in phosphate buffer at pH 7.4).

## Biodistribution in normal mice

Solutions of [$^{11}$C]-**10** or [$^{11}$C]-**12** obtained after RP-HPLC purification were diluted using water for injection to obtain an ethanol concentration < 5%, and further to a concentration of about 18.5 MBq/mL. The biodistribution of both tracers was determined in male NMRI mice (body weight 30–38 g). The animal studies were performed according to the Belgian code of practice for the care and use of animals, after approval from the university ethics committee for animals. A volume of 0.2 mL of the diluted tracer solution was injected into each mouse via a tail vein, under anesthesia (2.5% isoflurane in 100% $O_2$ at a flow rate of 1 L/min). The mice were sacrificed by decapitation at 2 min or 60 min after injection ($n = 3$ at each time point). Blood and major organs were collected in a tared tube after dissection and weighed. All organs and other body parts were measured for their radioactivity using a gamma counter. Results are expressed as %ID (cpm in organ/total cpm recovered), or, where possible, as SUVs. SUVs were calculated as (radioactivity in cpm in organ/weight of the organ in g)/(total counts recovered/body weight in g). For the calculation of total radioactivity in blood, blood mass was assumed to be 7% of the body mass.[26]

## Affinity of test compounds for nucleoside kinase enzyme VZV-TK *in vitro*

The 50% inhibitory concentration ($IC_{50}$) value of the synthesized compounds **9**–**12** against phosphorylation of [$CH_3$-$^3$H]dThd (deoxythymidine) as the natural substrate for VZV-TK was determined. Briefly, the activity of the purified recombinant VZV-TK enzyme was assayed in a 50-μL reaction mixture containing 50 mM Tris–HCl, pH 8.0, 2.5 mM $MgCl_2$, 10 mM dithiothreitol, 2.5 mM ATP, 1.0 mg/mL bovine serum albumin, 10 mM NaF, [$CH_3$-$^3$H]dThd (3.7 kBq in 5 μL; 1 μM final concentration) and 5 μL of a solution of recombinant enzyme (containing 7.75 ng of VZV-TK protein). The samples were incubated at 37°C for 30 min in the presence or absence of different concentrations of the test compounds. During this time period, the enzymatic reaction proceeded linearly. Aliquots of 45 μL of the reaction mixtures were spotted on Whatman DE-81 filter paper

disks (Whatman, Maidstone, UK). The filters were washed three times for 5 min in 1 mM ammonium formate and once for 5 min in ethanol. The radioactivity on the filters was determined by liquid scintillation counting.

## Conclusion

Carbon-11-labeled BCNAs without sugar moiety or with an acyclic sugar have been synthesized and evaluated for their affinity for VZV-TK *in vitro* and for their brain uptake in normal mice. Neither of the synthesized tracers was taken up in the brain. Both the acyclic and the ribose lacking derivative still showed moderate affinity for the VZV-TK. The results from our previous studies[18–21] and this study strongly suggest that bicyclic furopyrimidine system analogues (BCNAs) do not cross BBB and hence can be used for *in vivo* gene expression imaging outside of the brain only. This is an important insight into the structure–brain uptake relationship of this class of compounds as the *p*-pentylphenyl derivative is currently in the drug development phase for use in shingles infection.[28] Our experience with radiolabeled BCNAs suggests that a potential BCNA tracer for *in vivo* visualization of VZV-tk should have good affinity for the enzyme VZV-TK ($IC_{50}$ value ideally be $< 5\,\mu M$) and should have reasonable lipophilicity (log *P* value ideally be over 1) for a good accumulation in VZV-tk expressing cells.

## Acknowledgement

The technical assistance of Mrs Lizette van Berckelaer is gratefully acknowledged. We thank Peter Vermaelen, Humphrey Fonge and Li Xin Jin for their help during biodistribution studies. This work was supported by the SBO grant (IWT-30 238) of the Flemish Institute supporting Scientific-Technological Research in industry (IWT), the IDO grant (IDO/02/012) of the Katholieke Universiteit Leuven, in part by the European Commission (EC) – FP6-project DiMI, LSHB-CT-2005-512146, the R. Descartes-Prize-2001 of the EC (HPAW-2002-90001) and by the BioMacs of the Katholieke Universiteit Leuven.

## REFERENCES

[1] I. Penuelas, J. F. Boan, J. M. Marti-Climent, B. Sangro, G. Mazzolini, J. Prieto, J. A. Richter, *Mol. Imaging Biol.* **2004**, *6*, 225–238.
[2] S. S. Gambhir, *Nat. Rev. Cancer* **2002**, *2*, 683–693.
[3] I. Serganova, R. Blasberg, *Nucl. Med. Biol.* **2005**, *32*, 763–780.
[4] H. R. Herschman, *Crit. Rev. Oncol. Hematol.* **2004**, *51*, 191–204.
[5] M. M. Alauddin, P. S. Conti, S. M. Mazza, F. M. Hamzeh, J. R. Lever, *Nucl. Med. Biol.* **1996**, *23*, 787–792.
[6] M. M. Alauddin, P. S. Conti, *Nucl. Med. Biol.* **1998**, *25*, 175–180.
[7] J. G. Tjuvajev, M. Doubrovin, T. Akhurst, S. D. Cai, J. Balatoni, M. M. Alauddin, R. Finn, W. Bornmann, H. Thaler, P. S. Conti, R. G. Blasberg, *J. Nucl. Med.* **2002**, *43*, 1072–1083.
[8] M. M. Alauddin, A. Shahinian, R. Park, M. Tohme, J. D. Fissekis, P. S. Conti, *J. Nucl. Med.* **2004**, *45*, 2063–2069.
[9] S. Yaghoubi, J. R. Barrio, M. Dahlbom, M. Iyer, M. Namavari, R. Goldman, H. R. Herschman, M. E. Phelps, S. S. Gambhir, *J. Nucl. Med.* **2001**, *42*, 1225–1234.
[10] S. S. Yaghoubi, M. A. Couto, C. C. Chen, L. Polavaram, G. G. Cui, L. Y. Sen, S. S. Gambhir, *J. Nucl. Med.* **2006**, *47*, 706–715.
[11] C. McGuigan, C. J. Yarnold, G. Jones, S. Velazquez, H. Barucki, A. Brancale, G. Andrei, R. Snoeck, E. De Clercq, J. Balzarini, *J. Med. Chem.* **1999**, *42*, 4479–4484.
[12] C. McGuigan, H. Barucki, S. Blewett, A. Carangio, J. T. Erichsen, G. Andrei, R. Snoeck, E. De Clercq, J. Balzarini, *J. Med. Chem.* **2000**, *43*, 4993–4997.
[13] C. McGuigan, A. Brancale, H. Barucki, S. Srinivasan, G. Jones, R. Pathirana, A. Carangio, S. Blewett, G. Luoni, O. Bidet, A. Jukes, C. Jarvis, G. Andrei, R. Snoeck, E. De Clercq, J. Balzarini, *Antiviral Chem. Chemother.* **2001**, *12*, 77–89.
[14] J. Balzarini, C. McGuigan, *Biochim. Biophys. Acta-Mol. Basis Dis.* **2002**, *1587*, 287–295.
[15] J. Balzarini, C. McGuigan, *J. Antimicrob. Chemother.* **2002**, *50*, 5–9.
[16] R. Sienaert, L. Naesens, A. Brancale, E. De Clercq, C. McGuigan, J. Balzarini, *Mol. Pharmacol.* **2002**, *61*, 249–254.
[17] J. Balzarini, R. Sienaert, S. Liekens, A. Van Kuilenburg, A. Carangio, R. Esnouf, E. De Clercq, C. McGuigan, *Mol. Pharmacol.* **2002**, *61*, 1140–1145.
[18] S. K. Chitneni, C. M. Deroose, J. Balzarini, R. Gijsbers, S. J. L. Celen, T. J. de Groot, Z. Debyser, L. Mortelmans, A. M. Verbruggen, G. M. Bormans, *J. Med. Chem.* **2007**, *50*, 1041–1049.
[19] S. K. Chitneni, C. M. Deroose, J. Balzarini, R. Gijsbers, S. Celen, Z. Debyser, L. Mortelmans, A. M. Verbruggen, G. M. Bormans, *J. Med. Chem.* **2007**, *50*, 6627–6637.
[20] S. K. Chitneni, C. M. Deroose, H. Fonge, R. Gijsbers, N. Dyubankova, J. Balzarini, Z. Debyser, L. Mortelmans, A. M. Verbruggen, G. M. Bormans, *Bioorg. Med. Chem. Lett.* **2007**, *17*, 3458–3462.
[21] S. K. Chitneni, T. De Ruymaeker, J. Balzarini, A. M. Verbruggen, G. M. Bormans, *J. Labelled Compd. Radiopharm.* **2007**, *50*, 649–655.
[22] Z. Janeba, J. Balzarini, G. Andrei, R. Snoeck, E. De Clereq, M. J. Robins, *J. Med. Chem.* **2005**, *48*, 4690–4696.
[23] M. Ubasawa, H. Takashima, K. Sekiya, *Chem. Pharm. Bull.* **1995**, *43*, 142–143.
[24] D. D. Dishino, M. J. Welch, M. R. Kilbourn, M. E. Raichle, *J. Nucl. Med.* **1983**, *24*, 1030–1038.
[25] R. C. Young, R. C. Mitchell, T. H. Brown, C. R. Ganellin, R. Griffiths, M. Jones, K. K. Rana, D. Saunders, I. R. Smith, N. E. Sore, T. J. Wilks, *J. Med. Chem.* **1988**, *31*, 656–671.
[26] A. R. Fritzberg, W. P. Whitney, C. C. Kuni, W. Klingensmith, *Int. J. Nucl. Med. Biol.* **1982**, *9*, 79–82.
[27] P. H. Elsinga, N. H. Hendrikse, J. Bart, W. Vaalburg, A. van Waarde, *Curr. Pharm. Design* **2004**, *10*, 1493–1503.
[28] G. Luoni, C. McGuigan, G. Andrei, R. Snoeck, E. De Clercq, J. Balzarini, *Bioorg. Med. Chem. Lett.* **2005**, *15*, 3791–3796.